Mechanical properties of graphene under shear deformation

K. Min and N. R. Aluru[a)]
Department of Mechanical Science and Engineering, Beckman Institute for Advanced Science and Technology, University of Illinois at Urbana-Champaign, Urbana, Illinois 61801, USA

(Received 5 October 2010; accepted 7 December 2010; published online 7 January 2011)

In this letter, we investigate the mechanical properties of graphene under shear deformation. Specifically, using molecular dynamics simulations, we compute the shear modulus, shear fracture strength, and shear fracture strain of zigzag and armchair graphene structures at various temperatures. To predict shear strength and fracture shear strain, we also present an analytical theory based on the kinetic analysis. We show that wrinkling behavior of graphene under shear deformation can be significant. We compute the amplitude to wavelength ratio of wrinkles using molecular dynamics and compare it with existing theory. Our results indicate that graphene can be a promising mechanical material under shear deformation. © *2011 American Institute of Physics*.
[doi:10.1063/1.3534787]

Graphene has recently attracted significant attention from the scientific community because of its extraordinary mechanical and electrical properties. The attractive properties of graphene are currently being explored for a number of applications including nanoelectromechanical systems, nanoelectronics, etc. Recent mechanical experiments have shown that graphene is the strongest material measured so far.[1] This opens up opportunities for graphene as a nanomechanical material. The mechanical properties of graphene under tension have been investigated extensively using both experiments and atomistic simulation methods.[1–6] The shear modulus of graphene has been reported using various approaches. By using the molecular mechanics method, Sakhaee-Pour[7] reported the shear modulus of zigzag and armchair structures to be 0.213 and 0.228 TPa, respectively. Zakharchenko *et al.*[8] reported the temperature-dependent shear modulus using Monte Carlo simulation, and the highest value is 0.493 TPa at 700 K assuming the thickness of graphene to be 3.335 Å. Tsai *et al.* reported the shear modulus of graphene as 0.358 TPa at 0 K using molecular dynamics with AMBER force field.[9] Even though the shear modulus of graphene has been reported using several approaches, the strength and fracture strain of graphene under shear have not been reported so far.

To understand the merits and limitations of graphene as a mechanical material, it is important to look at shear properties of other materials. McSkimin and Andreatch[10] reported the shear modulus of diamond as 0.478 TPa. Roundy and Cohen[11] reported the shear strength of carbon diamond structure as 93 GPa. Zhang *et al.*,[12] using the first-principles approach and the local-density-approximation, reported the shear strength of c-BN and BC_2N-2 as 70.5 and 68.8 GPa, respectively. Shear modulus of graphite was reported to be 0.44 ± 0.03 TPa by Blakslee *et al.*[13] using experiments. For carbon nanotubes, Lu,[14] using empirical lattice dynamics, reported the shear modulus as 0.45 TPa, Hall *et al.*[15] reported the shear modulus using experiments as 0.41 ± 0.36 TPa, and Lu and Zhang[16] reported the shear strength to be between 41 and 54.4 GPa depending on the chirality. Since graphene is a thin membrane structure, it is also important to understand the wrinkling behavior under shear deformation. In related work, Wong and Pellegrino[17] studied the wrinkling behavior of aluminized Kapton membrane extensively using experiments, analytical and numerical simulations, and Wang *et al.*[18] investigated the wrinkling behavior of graphene under a point load.

In this paper, we perform extensive molecular dynamics simulations to understand the shear modulus, shear strength, and fracture strain of graphene as a function of temperature and chirality. Furthermore, we also investigate the wrinkling of graphene under shear deformation using molecular dynamics and analytical theory.[17] We also present an analytical theory based on the kinetic analysis to compute the shear strength and strain and compare the results with those obtained from molecular dynamics simulations. The rest of the paper contains details on molecular dynamics simulations, analytical theory based on kinetic analysis for fracture of graphene, and results on mechanical properties of graphene under shear deformation.

Molecular dynamics (MD) simulations are performed using large-scale atomic/molecular massively parallel simulator (Ref. 19) with the adaptive intermolecular reactive empirical bond order (AIREBO) potential.[20] It has been shown that the AIREBO potential can accurately compute the bond-bond interaction, bond breaking, and bond reforming in the carbon atoms.[6] To capture the fracture behavior accurately and to avoid nonphysical phenomenon, the cutoff parameter is modified as 2.0 Å for the REBO part of the potential.[21]

To compute the shear properties of bulk graphene, a total of 3936 carbon atoms with a size of 100.8×102.2 Å^2 and with periodic boundary conditions is initially relaxed using NPT simulation until the energy of the system is fully minimized for each specified temperature in the range of 100–2000 K. The thickness of graphene is assumed to be 3.335 Å. We implement the deformation-control method[6] by applying the shear strain rate of 0.001 ps^{-1} to bulk graphene (for both zigzag and armchair cases, separately). The strain increment is applied after every 1000 time steps using NVT simulation. The velocity-Verlet time stepping scheme is used with a time step of 0.1 fs and Nosé–Hoover thermostat is used for temperature control. Shear modulus, G, is computed using the expression

a)Author to whom correspondence should be addressed. Electronic mail: aluru@illinois.edu.

 © 2011 American Institute of Physics

Downloaded 07 Jan 2011 to 130.126.121.152. Redistribution subject to AIP license or copyright; see http://apl.aip.org/about/rights_and_permissions

TABLE I. Parameters for kinetic analysis.

	U_0 (eV)	V (Å^3)	a [10^{11} Pa]	b
Zigzag	1.85	4.69	0.44	9.3
Armchair	1.77	4.56	0.63	5.5

$$G = \frac{1}{V_0}\left(\frac{\partial^2 E}{\partial \gamma_{xy}^2}\right)_{\gamma_{xy}=0},$$

where E is the strain energy, V_0 is the volume, and shear strain $\gamma_{xy}=\Delta x/L$, where Δx is the transverse displacement and L is the initial length of graphene. To verify the shear modulus calculation, the linear portion of the shear stress and strain curve is used, $G=\tau_{xy}/\gamma_{xy}$, where τ_{xy} is the shear stress at 0.005 strain. This result is consistent with the result obtained from the strain energy based method described above.

The analytical theory employed here is based on the kinetic analysis of fracture. In kinetic analysis, the fracture of a material (lifetime of the fracture of a solid) is determined by two dominant factors, mechanical stress and temperature, i.e., $\tau=\tau_0 \exp(U_0-\beta\tau_{xy}/kT)$, where τ_0 is the vibration period of atoms in a solid, which is taken to be 10^{-13} s (Ref. 22), T is the temperature, U_0 is the interatomic bond dissociation energy, $\beta=$qV, where V is the activation volume and q is the coefficient of local overstress, and k is the Boltzmann constant. According to the Bailey criterion,[23] if the stress varies with time, the fracture is initiated when $\int_0^{t_f}(dt)/\tau[T,\tau_{xy}(t)]=1$, where t_f is the time to fracture and $\tau_{xy}(t)$ is the time-dependent stress.

To capture the nonlinear shear stress and strain behavior, a nonlinear expression relating shear stress to shear strain is employed, i.e., $\tau_{xy}(t)=a\ln[b\gamma_{xy}(t)+1.0]$. Assuming a constant strain rate, $\dot{\gamma}_{xy}$, the nonlinear stress-strain expression is given by

$$\tau_{xy}(t) = a\ln[b\dot{\gamma}_{xy}t + 1.0]. \quad (1)$$

Then, $\tau_f=a\ln[b\dot{\gamma}_{xy}t_f+1.0]$ is defined as the fracture stress. Substituting Eq. (1) and the expression for the life time (τ) into the Bailey criterion, we can obtain the temperature-dependent expression for fracture stress as

$$\tau_f(\dot{\gamma}_{xy},T) = \frac{akT}{\beta a + kT}\left\{\frac{U_0}{kT} + \ln\left[b\dot{\gamma}_{xy}\tau_0\left(\frac{\beta a}{kT}+1\right)\right]\right\}. \quad (2)$$

Furthermore, the expression for fracture strain is given by

$$\gamma_f = \frac{1}{b}\left[\exp\left(\frac{\tau_f}{a}\right) - 1.0\right]. \quad (3)$$

The interatomic bond dissociation energy, activation volume, and the parameters a and b do not vary significantly with temperature. The values used for these parameters for zigzag and armchair structures are summarized in Table I.

Shear stress as a function of shear strain for zigzag and armchair graphene are obtained for various temperatures. As shown in Fig. 1, for both armchair and zigzag cases, as the temperature increases, the shear modulus increases at first and then starts to decrease as the temperature increases beyond 800 K. As shown in inset 3 in Fig. 1, the anomalous variation of the shear modulus can be explained by the anomalous variation of the bond-length with temperature. As

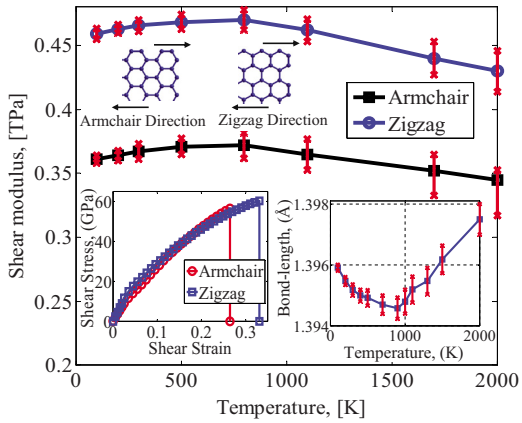

FIG. 1. (Color online) Chirality and temperature-dependent shear modulus. Inset 1 (top): armchair and zigzag graphene configuration for shear tests. Inset 2 (bottom-left): shear stress vs strain curve at 300 K. Inset 3 (bottom-right): first nearest C–C bond-length vs temperature.

the bond-length increases, the intermolecular interactions become weaker resulting in a decrease in shear modulus and vice versa. The bond-length variation with temperature is in reasonable agreement with the result obtained using Monte Carlo simulation.[8] Zigzag graphene shows a slightly higher shear modulus compared to the armchair graphene. As shown in inset 2 of Fig. 1, the shear stress versus strain curve shows a bifurcation point (change in slope) for a shear strain of around 0.024 for both chiralities. The critical shear stress when wrinkles appear at the bifurcation point is 10.5 and 8.7 GPa for zigzag and armchair structures, respectively, at 300 K. The decrease in slope represents a softening of the material (lower shear modulus). Beyond the bifurcation point, the wrinkles in the graphene membrane start to grow and the amplitude of the wrinkles becomes higher.

Since wrinkles can affect the mechanical behavior of graphene, we investigate the growth of wrinkles (in particular the amplitude and wavelength) under shear deformation. The ratio of the amplitude to the wavelength of wrinkles at various temperatures can be computed directly from the molecular dynamics data. In addition, the ratio can also be computed using theory[17] as

$$\frac{A}{\lambda} = \frac{\sqrt{2(1-\upsilon)\gamma_{xy}}}{\pi},$$

where A is the amplitude, λ is the half-wavelength, υ is Poisson's ratio, and γ_{xy} is the shear strain. For Poisson's ratio, we take a value of 0.21 ± 0.01 at 300 K,[6] 0.32 ± 0.08 at 800 K, and 0.34 ± 0.11 at 1700 K. We note that the ratio of the amplitude to the half-wavelength is not strongly dependent on the chirality of the graphene structure. This is reasonable because Poisson's ratio for both chiralities is approximately the same. The comparison between MD and theory is shown in Fig. 2. We note that the comparison is reasonable. Understanding the role of wrinkles is important, especially in a material like graphene, as wrinkles can lead to the softening of the material. To demonstrate the significance of wrinkles, we performed shear test on the zigzag graphene using molecular dynamics and preventing the formation of wrinkles by constraining the pressure component as zero in the z-direction. The fracture stress of a flat graphene sheet (with no wrinkles) is 97.54 GPa at 300 K, which is about 37 GPa higher when wrinkles are taken into account.

Downloaded 07 Jan 2011 to 130.126.121.152. Redistribution subject to AIP license or copyright; see http://apl.aip.org/about/rights_and_permissions

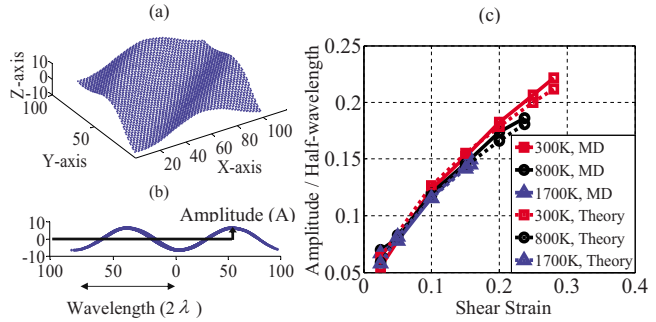

FIG. 2. (Color online) Wrinkle structures in grapheme. (a) Wrinkles in zigzag graphene at 0.2 strain, 300 K. (b) Side view of wrinkles. (c) Ratio of amplitude to half-wavelength vs shear strain at different temperatures for zigzag graphene and comparison with the analytical expression.

We also performed fracture simulations on zigzag and armchair graphene structures under shear deformation at various temperatures. The shear strength and shear fracture strain of armchair and zigzag structures as a function of temperature are shown in Fig. 3. We note that both the shear strength and the fracture strain decrease as temperature increases. The decrease in strength can be explained by larger thermal fluctuations at higher temperatures. The chirality effects are more clearly observed at lower temperature and are not that significant at higher temperatures. In particular, zigzag graphene shows a slightly higher strength at lower temperatures compared to the armchair graphene. We note that the fracture of graphene is initiated when the bonds along the north-west diagonal direction start to break because of the shear force. In Fig. 3, we also show the results from analytical theory based on kinetic analysis. While the results from the analytical theory compare reasonably well with MD data for both fracture stress and fracture strain, the chirality effects are not clearly observed with the analytical theory. Our

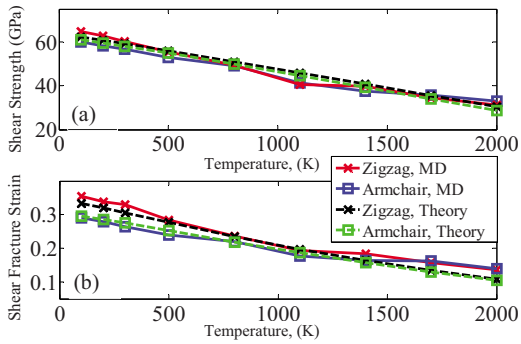

FIG. 3. (Color online) Chirality and temperature-dependent shear strength and shear fracture strain and comparison with kinetic analysis of the mechanism of fracture.

results indicate that the shear strength of graphene at 300 K is higher compared to that of the CNT case (41–54.4 GPa) (Ref. 16) and lower compared to that of carbon diamond (93 GPa),[11] c-BN (70.5 GPa), and BC_2N-2 (68.8 GPa).[12]

In summary, in this letter, we investigated the temperature and chirality dependent shear properties of graphene using molecular dynamics simulations. Our results indicate that shear modulus increases up to around 800 K and decreases as the temperature is increased further. Shear strength and fracture strain decrease as the temperature is increased. Zigzag graphene shows a higher shear modulus compared to the armchair structure. The shear fracture strength and shear fracture strain for the zigzag case are higher compared to the armchair case at lower temperatures, and no significant difference is observed at higher temperatures. We showed that analytical theory based on kinetic analysis compares reasonably with MD data. Finally, we also investigated wrinkling of graphene under shear deformation and since wrinkling can affect mechanical properties, this needs to be carefully accounted for when exploring applications based on graphene.

This work is supported by the National Science Foundation under Grant Nos. 0810294 and 0941497.

[1]C. Lee, X. Wei, J. W. Kysar, and J. Hone, Science **321**, 385 (2008).
[2]I. W. Frank, D. M. Tanenbaum, A. M. van der Zande, and P. L. McEuen, J. Vac. Sci. Technol. B **25**, 2558 (2007).
[3]F. Liu, P. Ming, and J. Li, Phys. Rev. B **76**, 064120 (2007).
[4]G. Van Lier, C. V. Alsenoy, V. V. Doren, and P. Geerlings, Chem. Phys. Lett. **326**, 181 (2000).
[5]H. Zhao, K. Min, and N. R. Aluru, Nano Lett. **9**, 3012 (2009).
[6]H. Zhao and N. R. Aluru, J. Appl. Phys. **108**, 064321 (2010).
[7]A. Sakhaee-Pour, Solid State Commun. **149**, 91 (2009).
[8]K. V. Zakharchenko, M. I. Katsnelson, and A. Fasolino, Phys. Rev. Lett. **102**, 046808 (2009).
[9]J. Tsai and J. Tu, Mater. Des. **31**, 194 (2010).
[10]H. J. McSkimin and P. Andreatch, J. Appl. Phys. **43**, 2944 (1972).
[11]D. Roundy and M. L. Cohen, Phys. Rev. B **64**, 212103 (2001).
[12]Y. Zhang, H. Sun, and C. Chen, Phys. Rev. Lett. **93**, 195504 (2004).
[13]O. L. Blakslee, D. G. Proctor, E. J. Seldin, G. B. Spence, and T. Weng, J. Appl. Phys. **41**, 3373 (1970).
[14]J. P. Lu, Phys. Rev. Lett. **79**, 1297 (1997).
[15]A. R. Hall, L. An, J. Liu, L. Vicci, M. R. Falvo, R. Superfine, and S. Washburn, Phys. Rev. Lett. **96**, 256102 (2006).
[16]J. Lu and L. Zhang, Comput. Mater. Sci. **35**, 432 (2006).
[17]Y. W. Wong and S. Pellegrino, J. Mech. Mater. Struct. **1**, 25 (2006).
[18]C. Y. Wang, K. Mylvaganam, and L. C. Zhang, Phys. Rev. B **80**, 155445 (2009).
[19]S. J. Plimpton, J. Comput. Phys. **117**, 1 (1995).
[20]S. J. Stuart, A. B. Tutein, and J. A. Harrison, J. Chem. Phys. **112**, 6472 (2000).
[21]T. Belytschko, S. P. Xiao, G. C. Schatz, and R. Ruoff, Phys. Rev. B **65**, 235430 (2002).
[22]S. N. Zhurkov, Int. J. Fract. Mech. **1**, 311 (1965).
[23]J. Bailey, Glass Ind. **20**, 26 (1939).

Downloaded 07 Jan 2011 to 130.126.121.152. Redistribution subject to AIP license or copyright; see http://apl.aip.org/about/rights_and_permissions